

Morphology and Structure of ZnO Nanoparticles Produced by Electrochemical Method

Barbara STYPUŁA, Angelika KMITA*, Michał HAJOS

AGH University of Science and Technology, Faculty of Foundry Engineering, Reymonta St. 23, 30-059 Krakow, Poland

crossref <http://dx.doi.org/10.5755/j01.ms.20.1.4417>

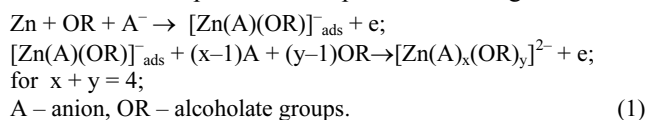
Received 21 May 2013; accepted 23 January 2014

This article presents studies of the morphology and structure of ZnO nanoparticles synthesized by the electrochemical method. Colloidal solutions of the nanoparticles are obtained by an anodic dissolution of metallic zinc in alcohol solutions of lithium chloride containing a small amount of water (5 % vol.). The parameters chosen for the synthesis are based on Zn polarization curves (obtained using the potentiokinetic (Linear Sweep Voltammetry – LSV) and the chronoamperometric method). The synthesis of zinc oxide nanoparticles is carried out in 0.05m LiCl + 5 % H₂O alcohol (methanol or propanol) solutions during galvanostatic polarization of Zn at 3 mA/cm² current density. The process is performed in a two-electrode system, where both electrodes (the working anode and cathode) are made of zinc. Optical properties, morphology and structure of the colloidal solutions and powders (obtained after evaporating the solvent) were studied using the following spectroscopic and microscopic techniques: UltraViolet and Visible Spectroscopy (UV-VIS), Fourier Transform Infrared Spectroscopy (FTIR), Scanning Electron Microscopy (SEM) and Transmission Electron Microscopy (TEM).

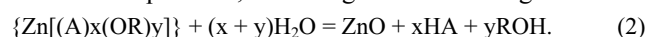
Keywords: ZnO nanoparticles, ZnO electrochemical synthesis, structure of colloidal ZnO.

1. INTRODUCTION

Due to unique electrical, photo-optical properties and chemical activity, ZnO nanoparticles have several applications, among others, including: production of catalysts, electrodes for photoelectrochemical cells, gas sensors, ultraviolet filters, and various nanocomposites. There are several methods of obtaining nanoparticles, namely: by thermal decomposition of precursors (salts) in a solid state, Chemical Vapor Deposition (CVD) technique, laser evaporation [1, 2], solution deposition or in a solvothermal way from over-saturated salt solutions in various solvents in the precipitated and/or hydrolysis process [3–5]. In recent times electrochemical methods have often been applied. [6–17]. The electrochemical method used by the authors, is based on an anodic dissolution of zinc in alcohol electrolytes [7]. Electrochemical behavior of zinc in alcohol solutions of salt [7, 10, 12, 15–17] indicated that Zn – at high anodic potentials – dissolves passing through the electrolyte in the form of soluble complexes with the participation of anion and solvent. The process takes place in two stages:



In electrolytes containing water, the decomposition (hydrolysis) of these complexes may occur with formation of ZnO nanoparticles, according to the following reaction:



Process pathways, both anodic dissolution and hydrolysis, depend mainly on the environment (the type of solvent, concentration of salt and water). Our study shows the morphology and structure of ZnO nanoparticles

obtained in 0.05m solution of LiCl in methanol and propanol containing 5 % vol. water.

2. METHODOLOGY OF INVESTIGATIONS

The synthesis of zinc oxide (ZnO) nanoparticles is carried out in 0.05m LiCl + 5 % H₂O alcohol solutions during anodic dissolution of metallic zinc under galvanostatic polarization – at a current density of 3 mA/cm². The synthesis is performed in a two-electrode system, where both electrodes (the working anode and cathode) are made of zinc. The parameters for the process are chosen based on polarization curves obtained using both the potentiokinetic (Linear Sweep Voltammetry – LSV) and the chronoamperometric method.

Before polarization the surfaces of samples (electrodes) are cleaned with a grade P800 to P1200 sandpaper, then rinsed with distilled water and alcohol.

Structure and properties of colloidal solutions of nanoparticles are investigated by means of UV-VIS – Ultra-Violet and Visible Spectroscopy – Perkin Elmer Lambda 25 UV-VIS Spectroscopy, FTIR – Fourier Transform Infrared spectroscope – Thermo Scientific Nicolet 6700 and Zetasizer Nano ZS nanosizer.

Composition, size and structures of nanopowders (after solvent evaporation) were investigated by means of electron microscope: JEOL JSM 5500 LV SEM with Energy Dispersive X-ray (EDX) microanalyser, ECNAI FEG SUPERTWIN (200kV) TEM and High-Resolution TEM (HRTEM).

3. RESULTS

3.1. Synthesis, morphology and structure of ZnO nanoparticles

Fig. 1 presents LSV polarization curves of zinc in methanol solutions of lithium chloride. There are two

*Corresponding author. Tel.: +48-12-6174551, fax: +48-12-6333348. E-mail address: akmita@agh.edu.pl (A. Kmita)

characteristic sections visible on the curves which confirm the two-phase course of the anodic process. There is the first low anodic potential region and the second steep one – above -1.0 V. Intensive dissolution of zinc in the form of complexes $[\text{Zn}(\text{A})_x\text{OR}]_y^{2-}$ occurs in the second section [15, 17]. The density of the anodic current increases in this region with the rise of concentration of chloride anions. The fractional order of reaction in relation to chloride anions [17] confirms that apart from Cl^- anions it is also the solvent that takes part in an anodic dissolution process. Zn polarization curves in the propanol solution (Fig. 2) take a similar course as in the methanol one. They only differ with respect to the values of the anodic current. Much lower current density in the LiCl propanol solution is related to conductivity of this solution and its higher polarization resistance. The addition of water induces the increase of the dissolution rate of zinc in the propanol electrolyte, Fig. 2. The influence of water content on the anodic current density at constant potential, -0.5 V (during chronoamperometric polarization of Zn) in methanol and propanol electrolyte is shown in Fig. 3 and Fig. 4, respectively.

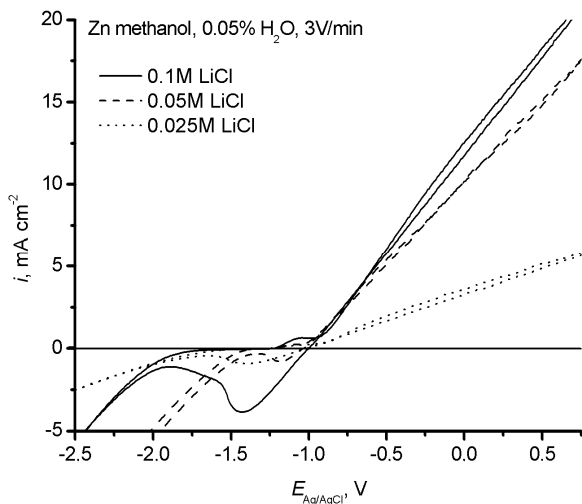


Fig. 1. LSV polarization curves of zinc in methanol solutions of lithium chloride

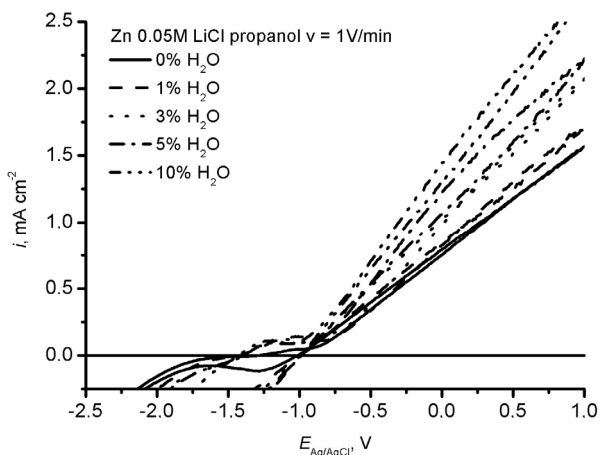


Fig. 2. LSV polarization curves of zinc in propanol solutions of lithium chloride

One can see irregular changes of current density (i) for Zn in the methanol electrolyte with increasing water concentration from 1 % vol. to 10 % vol., Fig. 3. It indicates a change of structure with regards to the properties of the products of anodic oxidation with a change of water concentration in the methanol solvent. A more regular dependence of the anodic current density on water concentration can be observed in the case of propanol electrolyte (Fig. 4). This density increases with an increased water content at $c_{\text{H}_2\text{O}} > 1$ %. It suggests that the increase of the zinc dissolution rate with the increase of water content in propanol electrolyte is caused by the rise of solubility of the products of anodic oxidation of zinc.

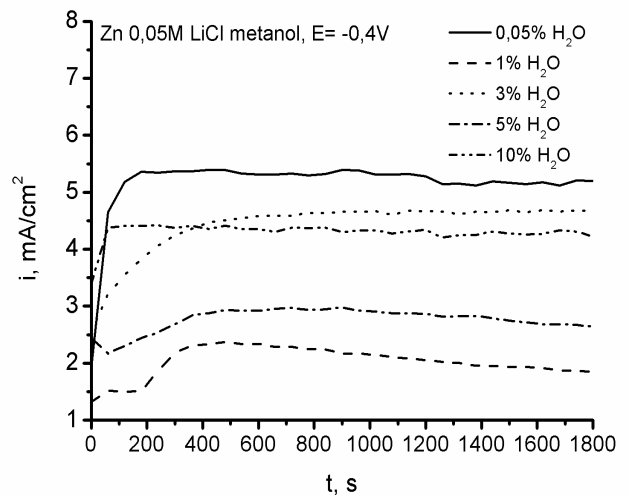


Fig. 3. Chronoamperometric polarization curves for zinc in methanol electrolytes, influence the concentration of water

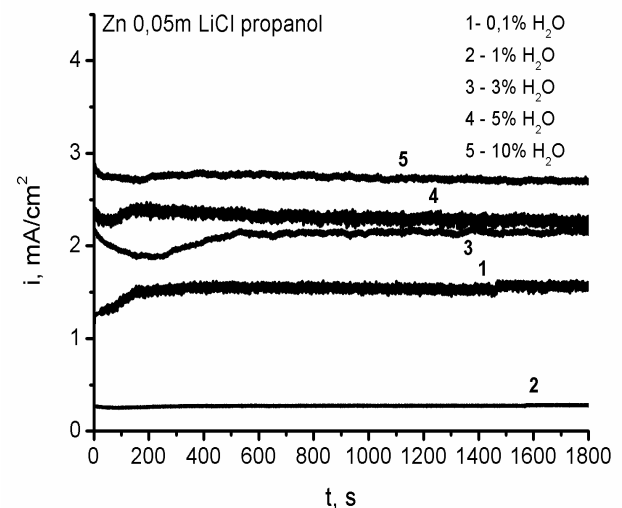


Fig. 4. Chronoamperometric polarization curves for zinc in propanol electrolytes, influence the concentration of water

Concentrations of chloride ions and water do not only influence the anodic dissolution rate of Zn, but also the chemical composition and structure of oxidation products as well as the hydrolysis of these products. This is confirmed by the examination of the absorption spectra (UV-VIS) of colloidal solutions (Fig. 5, a, b) and by the results of nanopowders tested after solvent evaporation, by

means of microscopic techniques (SEM/EDX, TEM, HRTM) and electron diffraction.

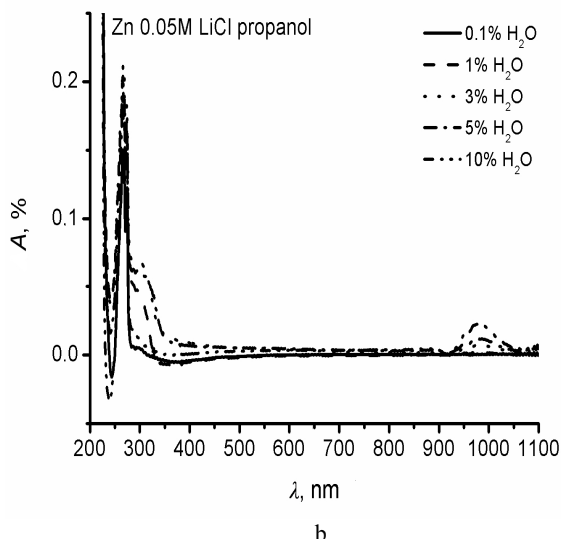
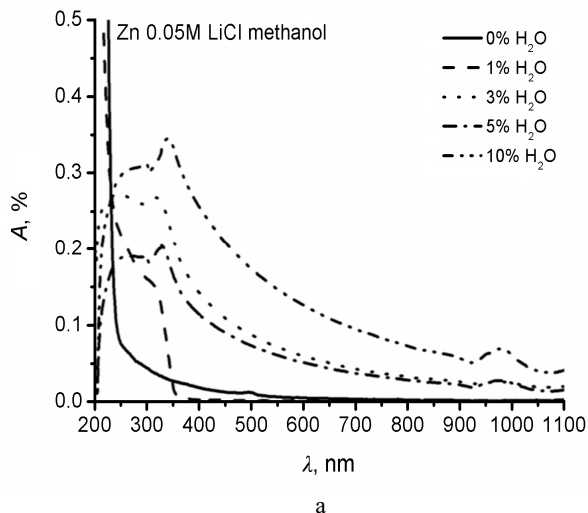


Fig. 5. Absorption spectrum of anolyte, $E = -0.4$ V, $t = 0.5$ h; a – in methanol; b – in propanol

According to literature, the absorption peak at wave length of app. 320 nm–360 nm corresponds to colloidal ZnO solutions [5, 18]. This peak is clearly visible in both alcohols in 0.05m LiCl containing 5%. The presence of zinc oxide (ZnO) in electrolytes containing 5% vol. H_2O in colloidal solutions is confirmed by X-ray diffraction results (XRD) [12], SEM/EDX (Figs. 6, 7), HRTM analysis (Figs. 8, 9), and electron diffraction (Figs. 10, 11).

The microanalysis of chemical composition of both powders indicate that the material contains mainly zinc and oxygen with a small amount of chlorine. Copper, which is also visible, originates from a net on which a drop was placed. TEM investigations, high resolution TEM and electro-diffraction pointed out that ZnO particles of plate-agglomerate shape of dimensions < 50 nm in methanol electrolyte and < 20 nm in propanol electrolyte have crystalline structures (Figs. 8–9, Figs. 10–11). Interplanar distances corresponding to ring radii seen in diffractions are relatively well matched with ZnO phases.

Table 1 show dimensions of ZnO (powders) observed by the transmission microscope (TEM) and colloidal solution determined by means of the ZetaSizer.

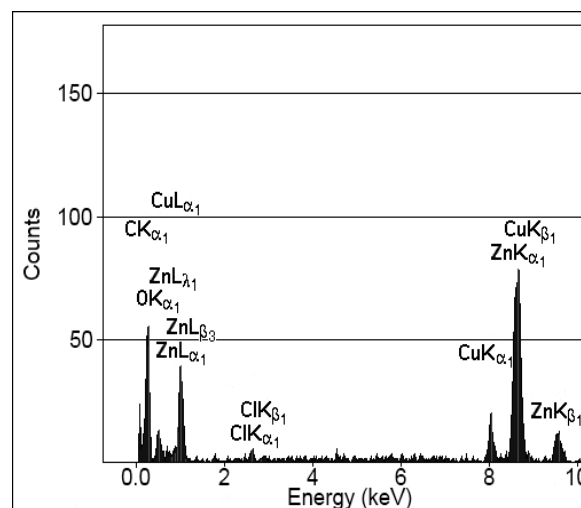
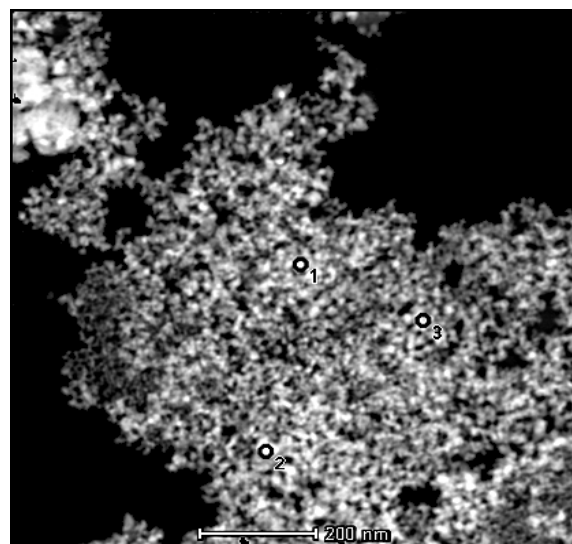
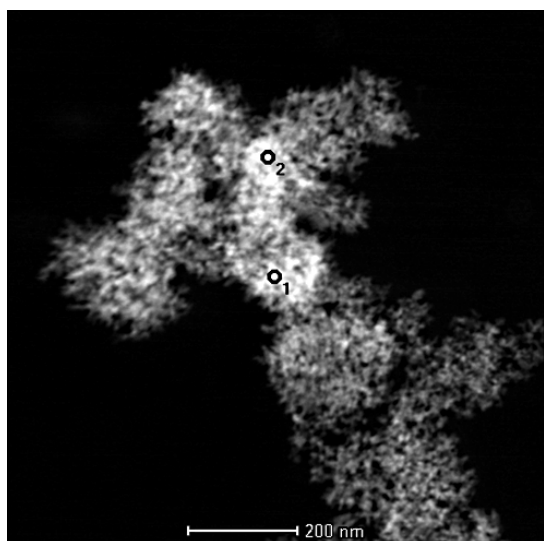


Fig. 6. Scanning-transmission microstructure ZnO nanopowder obtained in a methanol electrolyte (a), EDX spectrum of point '1' (b)

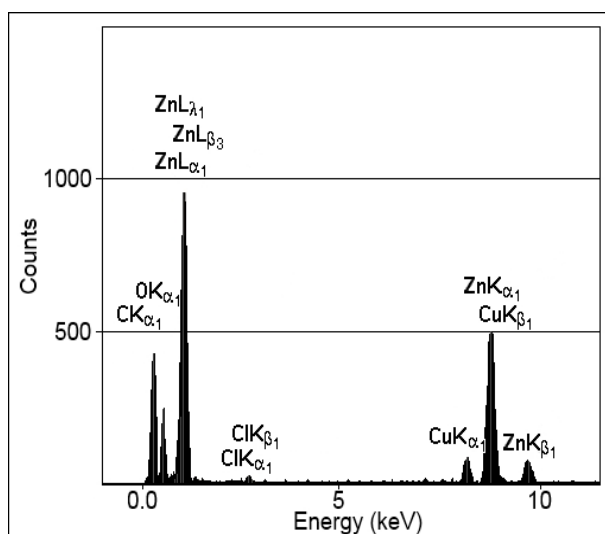
Table 1. Complete list of the investigation results obtained for colloidal solutions in methanol and propanol

Zn 0.05m LiCl methanol + 5% H_2O , $i = 3$ mA/cm ² (crystalline ZnO)		
	methanol	propanol
Size ZnO (powder) TEM [nm]	< 50 nm	< 20 nm
Size ZnO (in colloidal) ZetaSizer [nm]	~ 400 nm	~ 200 nm
Electrokinetic potential ζ [mV]	-9.45 ± 0.75	-13.65 ± 1.25

Dimensions of nanoparticles determined by means of the ZetaSizer are of one order of magnitude larger than dimensions observed by a transmission microscope (TEM)



a



b

Fig. 7. Scanning-transmission microstructure ZnO nanopowder obtained in a propanol electrolyte (a); EDX spectrum of point '1' (b)

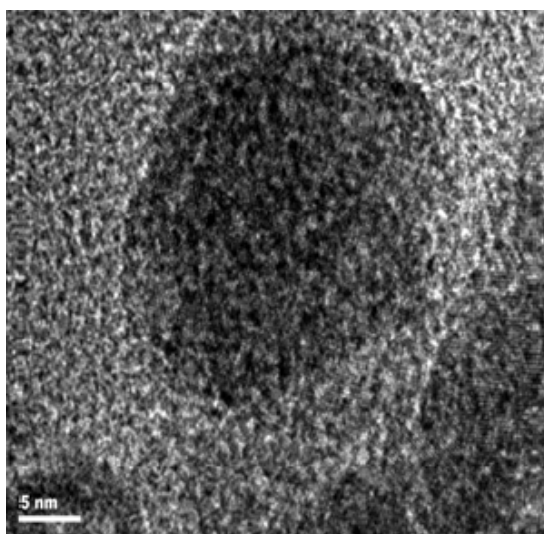


Fig. 8. HRTEM nanograph of the powder obtained in methanol electrolyte

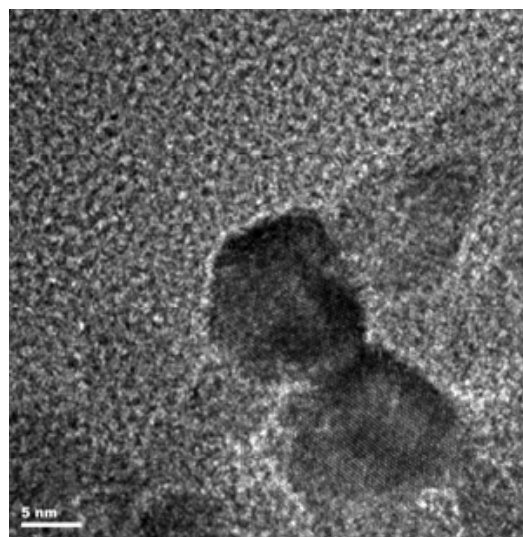
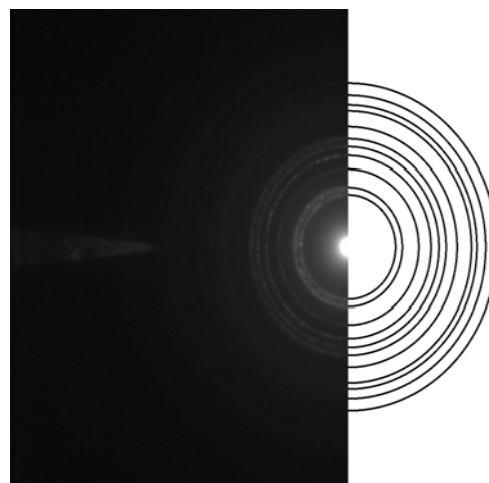


Fig. 9. HRTEM nanograph of the powder obtained in propanol electrolyte



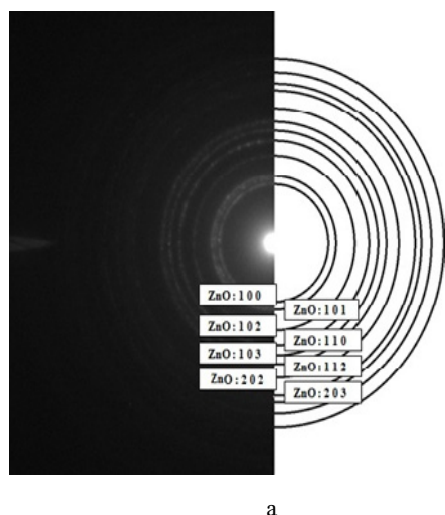
a

Sample (5 % H ₂ O)	ZnO		
	d (Å)	hkl	
d (Å)	2.829	2.817	100
	2.517	2.478	101
	1.914	1.913	102
	1.635	1.626	110
	1.482	1.478	103
	1.375	1.380	112
	1.242	1.239	202
	1.092	1.090	203

b

Fig. 10. Electron diffraction of ZnO obtained in methanol electrolyte (a) and tabular values of interplanar distances corresponding to these rings (b)

(Table 1). Several effects can be the reasons of the following differences: different structures of powder and particles in a colloidal system (ZnO nucleus and micelle) and, among others, limited accuracy of the DLS (Dynamic Light Scattering) measuring technique in the ZetaSizer.



Sample (5 % H ₂ O)	ZnO	
	d (Å)	hkl
d (Å)	2.817	100
	2.482	101
	1.904	102
	1.619	110
	1.473	103
	1.371	112
	1.230	202
	1.089	203

b

Fig. 11. Electron diffraction of ZnO obtained in propanol electrolyte (a) and tabular values of interplanar distances corresponding to these rings (b)

3.2. Characteristic by means of infrared spectroscopy – FTIR of colloidal ZnO solutions

Fig. 12. presents the absorption FTIR spectra of the colloidal solution of zinc oxide in methanol. Nanocrystalline zinc oxide, has a characteristic absorption band at wave numbers: (435–544) cm⁻¹, related to stretching vibrations in Zn–O [18–20]. For pure ZnO this band shifts in the direction of higher wave numbers, to app. 600 cm⁻¹ [21]. In the IR spectrum of colloidal suspension in methanol the band originated from ZnO is overlapped by a weak and broad absorption band originated from alcohol: 880 cm⁻¹–400 cm⁻¹, assigned to bending vibrations in OH group (with a maximum at app. 660 cm⁻¹) [22].

In the case of colloidal solutions (Fig. 12), certain differences between spectra of alcohol and of colloidal solution of nanoparticles in alcohol are seen. These differences mainly concern zones related to OH groups in alcohol and water particles (taking part in hydrogen bonds, –OH – O–H).

The band characteristic for alcohol, (3600–3100) cm⁻¹ with a maximum at 3352 cm⁻¹, becomes wider and shifts in the direction of lower wave numbers, Fig. 12, Table 2. This indicates the formation of hydrogen bonds at the interface between alcohol and oxide.

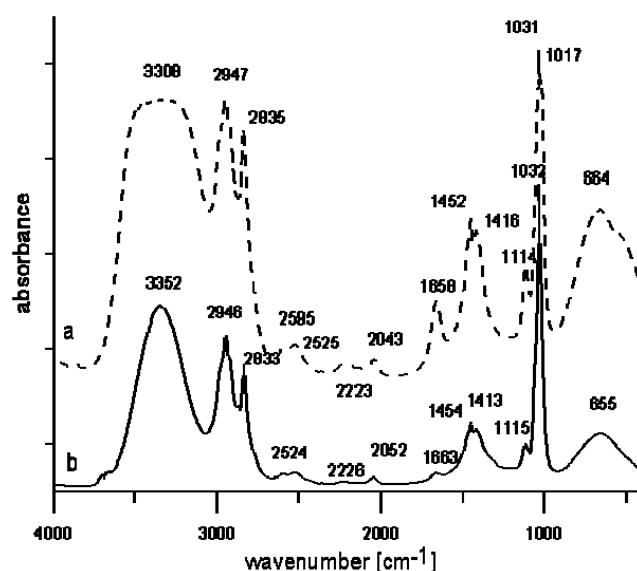


Fig. 12. FTIR spectra: a – ZnO in methanol, b – methanol

Table 2. Characteristic bands (peaks) in the FT-IR spectra for alcohols and water

Wave number [cm ⁻¹]	Group, kind of vibrations	Reference
3600–3200 3500–3000	vOH, vH ₂ O (stretching vibrations), v OH bound with hydrogen bridges vOH in alcohols	[23] [24] [25] [26][34]
1595	v ₂ , H ₂ O	[21]
1630	H ₂ O deformation vibrations of water inside complex	[27]
1642	Chemically bound water	[28]
3000–2850	C–H, stretching vibrations in alkanes	[24]
2922, 2854	v _s , v _{as} symmetric and asymmetric CH ₃ groups	[29]
1480–1350	–C–H, various deformation vibrations in alkanes	[24]
1300–1000	C–O in alcohols	[24]
2850, 2940	CH ₃ vs, v _a	[26]
1033	v CO in methanol	[30]
1115	OCH ₃	[31]
2570–2100	Various bonds related to absorption X–H, where X– can be C	[32]

In addition, a more intensive band at wave number 1115 cm⁻¹, originated from the OCH₃ methoxyl group and the remaining bands originated from bending vibrations of the CH₃ and CO group in the (2045–2950) cm⁻¹ range, as well as the band at 1658 cm⁻¹ being in the vicinity of 1642 cm⁻¹ corresponding to chemically bonded water (Fig. 12, Table 2) [23–32] – are all worth mentioning. According to [29], the shifting of the band originated from stretching vibrations in OH group, in the direction of lower wave numbers and especially the intensive increase of the band originated from OCH₃ indicates weakening of the O–H bond and the alcohol dissociation.

The observed changes in the analyzed spectra are mainly due to the alcohol adsorption on the surface of oxide nanoparticles, acid-base interaction (Lewis), alcohol – oxide interactions and the alcohol dissociation on ZnO nanoparticles surfaces followed by the adsorption of the products of this dissociation.

Smaller changes in spectra are seen in the case of ZnO suspension in propanol electrolyte (Fig. 13). It only indicates the alcohol adsorption on oxide nanoparticles. This is understandable, since propanol is a weaker protonic acid, (pK_s : 16.7 and 19.3 for methanol and propanol respectively) [33].

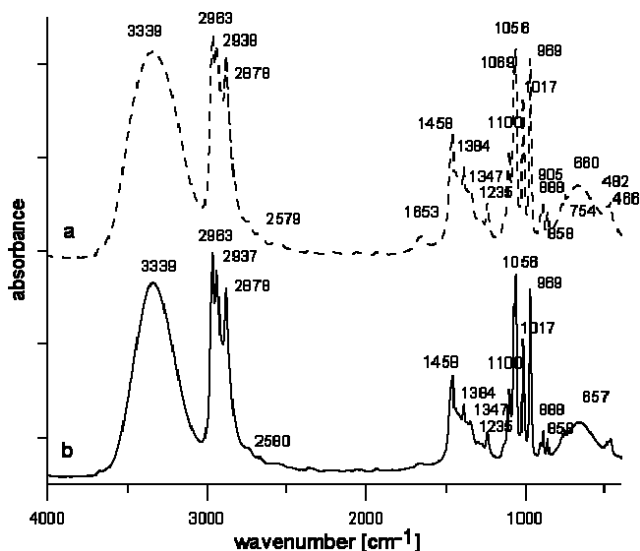


Fig. 13. Spectral FTIR analysis of colloidal ZnO in propanol (a) and spectra of propanol (b)

The FTIR spectra analysis of colloidal solutions of zinc oxide nanoparticles indicates the structure reorganization on the interface boundary: alcohol-oxide, caused by alcohol adsorption, and interactions of acid-base type (Lewis) [31, 33, 35]. As a consequence of these interactions is dissociation of alcohols, alcoxide formation or/and rehydrogenation of the oxide surface.

The degree and direction of surface structure changes depends on donor acceptor (acid-base) oxides as well as on alcohols properties. From the investigated colloidal ZnO suspensions larger changes in surface structures are observed in methanol colloids due to the solvent.

CONCLUSIONS

ZnO nanoparticles obtained by electrochemical dissolution of zinc in electrolytes (0.05m LiCl + 5 % vol. H₂O) with alcohol solvents have a crystalline structure. Nanoparticle dimensions depend on the type of alcohol. The sizes of nanoparticles after solvent evaporation are ~50 nm (in methanol) and 20 nm (in propanol). Colloidal micelles (in nanoparticle solutions) determined by the nanosizer method are equal to approximately 600 nm and 400 nm – respectively.

These particles in colloidal solutions obtain small negative electrokinetic potential ζ , caused by adsorption of alcohol and alcoxide group OR⁻. Methanol undergoes

dissociation to a higher degree than propanol. Apart from methanol, OCH₃ groups are also strongly adsorbed on ZnO. This is confirmed by stronger absorption bands in the FT-IR spectra within zones: (1000–1120) cm⁻¹ and (1600–2600) cm⁻¹ and a significantly broader band in the zone corresponding to OH groups (bonded by hydrogen bonds (3000–3600) cm⁻¹).

REFERENCES

1. Maruyama, T. Copper Oxide Thin Films Prepared by Chemical Vapor Deposition from Copper Dipivaloylmethanate *Solar Energy Materials and Solar Cells* 56 1998: pp. 85–92.
2. Nuñez-Sanchez, S., Serna, R., Petford-Long, A. K., Tanase, M. The Role of the Laser Fluence on the Al₂O₃ Target in the Nanostructure and Morphology of VO_x:Al₂O₃ Thin Films Prepared by Pulsed Laser Deposition *Applied Surface Science* 254 (4) 2007: pp. 1316–1321.
3. Lincot, D. Solution Growth Of Functional Zinc Oxide Films And Nanostructures *MRS Bulletin* 35 2010: pp. 778–789. <http://dx.doi.org/10.1557/mrs2010.507>
4. Wang, C., Hu, Y., Yan Shao, G. A Novel Method to Prepare Nanocrystalline SnO₂ *Nanostructure Materials* 6 1996: pp.421–427.
5. Wang, H., Xie, Ch., Zeng, D. J. Controlled Growth of ZnO by Adding H₂O *Crystal Growth* 277 2005: pp. 372–377.
6. Peulon, S., Lincot, D. Cathodic Electrodeposition from Aqueous Solution of Dense or Open-Structured Zinc Oxide Films *Advanced Materials* 2 1996: pp. 166–170. <http://dx.doi.org/10.1002/adma.19960080216>
7. Stypuła, B., Banaś, J., Habdank-Wojewódzki, T., Krawiec, H., Starowicz, M. Granted Patent Number P-369 320, 28.07.2004.
8. Stypuła, B., Banaś, J., Krawiec, H., Starowicz, M., Habdank-Wojewódzki, T., Janas, A. Anodic Dissolution of Copper in Organic Solvents as a Method for Obtaining Nanoparticles of Copper *Corrosion Protection* 11s/A 2004: pp. 25–29.
9. Gao, Y.-F., Nagai, M., Masuda, Y., Sato, F., Koumoto, K. Electrochemical Deposition of ZnO Film and Its Photoluminescence Properties *Journal of Crystal Growth* 286 2006: pp. 445–450.
10. Starowicz, M., Stypuła, B., Krawiec, H., Banaś, J. The Use of Metal Electrode Processes in Alcoholic Solutions of Electrolytes for the Preparation of Nanoparticles of Metal Oxides *Corrosion Protection* 11s/A 2005: pp. 25–30.
11. Stypuła, B., Banaś, J., Starowicz, M., Krawiec, H., Bernasik, A., Janas, A. Production of Nanoparticles of Copper Compounds by Anodic Dissolution of Copper in Organic Solvents *Journal Applied Electrochemistry* 36 2006: pp. 1407–1414.
12. Starowicz, M., Stypuła, B. Electrochemical Synthesis of ZnO Nanoparticles *European Journal of Inorganic Chemistry* 6 2008: pp.869–872. <http://dx.doi.org/10.1002/ejic.200700989>
13. Starowicz, M., Stypuła, B., Banaś, J. Electrochemical Synthesis of Silver Nanoparticles *Electrochemistry Communications* 8 2006: pp.227–230.
14. Starowicz, M., Sojka, A., Stypuła, B. Influence of Electrolyte on a Composition and Size of Copper Compound Particles *Archives of Materials Science and Engineering* 28 2007: pp. 609–612.

15. **Stypuła, B., Starowicz, M., Banaś, J.** Application of Anodic Dissolution of Metals for Nanoparticles Synthesis *Corrosion Protection* 49/11s/A 2006: pp.33–36.
16. **Banaś, J., Stypuła, B., Banaś, K., Światłowska-Mrowiecka, J., Starowicz, M., Lelek-Borkowska, U.** Corrosion and Passivity of Metals in Methanol Solutions of Electrolytes *Journal of Solid State Electrochemistry* 13 2009: pp. 1669–1679.
<http://dx.doi.org/10.1007/s10008-008-0649-5>
17. **Stypuła, B., Starowicz, M., Hajos, M., Olejnik, E.** Electrochemical Synthesis of ZnO Nanoparticles during Anodic Dissolution of Zinc in Alcohols Solvents *Archives of Metallurgy and Materials* 56 2011: pp. 287–292.
18. **Chin-Hsien Hung, Wha-Tzong Whang.** A Novel Low-Temperature Growth and Characterization of Single Crystal ZnO Nanorods *Materials Chemistry and Physics* 82 2003: pp. 705–710.
[http://dx.doi.org/10.1016/S0254-0584\(03\)00331-6](http://dx.doi.org/10.1016/S0254-0584(03)00331-6)
19. **Peng, X., et al.** Preparation and Optical Properties of ZnO@PPEGMA Nanoparticles *Applied Surface Science* 58 2009: pp. 7158–7163.
<http://dx.doi.org/10.1016/j.apsusc.2009.03.050>
20. **Kajbafvala, A., et al.** Nanostructure Sword-Like ZnO Wires: Rapid Synthesis and characterization Through a Microwave-Assisted Route *Journal of Alloys and Compounds* 469 2009: pp. 293–297.
<http://dx.doi.org/10.1016/j.jallcom.2008.01.093>
21. **Muthukumar, S., et al.** Structural, Optical and Photoluminescence Studies of Heavily Mn-Doped ZnO Nanoparticles Annealed under Ar Atmosphere *Journal of Materials Science: Materials in Electronics* 23/7 2012: pp. 1393–1401.
<http://dx.doi.org/10.1016/j.jallcom.2008.01.093>
22. **Natal-Santiago, M. A., Dumesic, J. A.** Microcalorimetric, FTIR, and DFT Studies of the Adsorption of Methanol, Ethanol, and 2,2,2-Trifluoroethanol on Silica *Journal of Catalysis* 75 1998: pp. 252–268.
23. **Martínez, E., et al.** Identification of Tetrahedral Sites and ²⁹Si NMR Lines of Silicalite from Molecular Dynamics *Chemical Physics Letters* 349 (3–4) 2001: pp. 286–290.
24. **Ramos-Tejada, M. M.** Investigation of Alumina(+)-Catechin System Properties. Part I: A Study of the System by FTIR-UV-VIS Spectroscopy *Colloids and Surfaces* 24 2002: pp. 297–308.
[http://dx.doi.org/10.1016/S0927-7765\(01\)00284-3](http://dx.doi.org/10.1016/S0927-7765(01)00284-3)
25. **Schroeder, P.** Infrared Spectroscopy in Clay Science *Teaching Clay Science* A.11 2002: pp. 181–187.
26. **Liu, F., et al.** In Situ Transmission Difference FTIR Spectroscopic Investigation on Anodic Oxidation of Methanol in Aqueous Solution *Electrochemistry Communications* 5 2003: pp. 276–282.
27. **Milka, R., et al.** Impedance Spectroscopic Investigation of the Effect of Thin Azo-calix[4]arene Film Type on the Cation Sensitivity of the Gold Electrodes *Materials Science and Engineering C* 30 2010: pp. 1466–1471.
28. **Potapova, E., et al.** The Effect of Polymer Adsorption on the Wetting Properties of Partially Hydrophobized Magnetite *Journal Colloid Interface Science* 367 2011: pp. 478–484.
29. **Lu, Y, Miller, J. D.** Carboxyl Stretching Vibrations of Spontaneously Adsorbed and LB-Transferred Calcium Carboxylates as Determined by FTIR Internal Reflection Spectroscopy *Journal of Colloid Interface Science* 256 2002: pp. 41–52.
<http://dx.doi.org/10.1006/jcis.2001.8112>
30. **Herzberg, G.** Molecular Electronic Spectra *Annual Review of Physical Chemistry* 2 1951: pp. 315–338.
31. **Bailly, M., et al.** A Spectroscopy and Catalysis Study of the Nature of Active Sites of MgO Catalysts: Thermodynamic Brønsted Basicity Versus Reactivity of Basic Sites *Journal of Catalysis* 235 2005: pp. 413–422.
32. **Martra, G., et al.** Surface Morphology and Reactivity of Microcrystalline MgO: Single and Multiple Acid-Base Pairs in Low Coordination Revealed by FTIR Spectroscopy of Adsorbed CO, CD₃CN and D₂ *Catalysis Today* 70 2001: pp. 121–130.
[http://dx.doi.org/10.1016/S0920-5861\(01\)00412-6](http://dx.doi.org/10.1016/S0920-5861(01)00412-6)
33. **Wigdorowicz, W. I., Cygankowa, L. E.** Anodic Behavior of Metals in acids with an Alcoholic Solvent. Moscow, Radiotechnika, 2009 (in Russian).
34. **Bobrowski, A., Stypuła, B., Hutera, B., Kmita, A., Drożyński, D., Starowicz, M.** FTIR Spectroscopy of Water Glass – the Binder Moulding Modified by ZnO Nanoparticles *Metalurgija – Metallurgy* 51/4 2012: pp. 477–480.
35. **Chizallet, C., et al.** Thermodynamic Bronsted Basicity of Clean MgO Surfaces Determined by Their Deprotonation Ability: Role of Mg²⁺-O²⁻ Pairs *Catalysis Today* 116/2 2006: pp 196–205.
<http://dx.doi.org/10.1016/j.cattod.2006.01.030>